International Journal of Heat and Mass Transfer 52 (2009) 2815–2823

Contents lists available at ScienceDirect

International Journal of Heat and Mass Transfer

journal homepage: www.elsevier.com/locate/ijhmt

Darcy–Benard–Marangoni convection in porous media

I.S. Shivakumara [a,*], C.E. Nanjundappa [b], Krishna B. Chavaraddi [c]

[a] UGC-Centre for Advanced Studies in Fluid Mechanics, Department of Mathematics, Bangalore University, Central College Campus, Bangalore 560 001, India
[b] Department of Mathematics, Dr. Ambedkar Institute of Technology, Bangalore 560 056, India
[c] Department of Mathematics, Manipal Institute of Technology, Manipal 576 104, India

ARTICLE INFO

Article history:
Received 7 May 2007
Received in revised form 18 September 2008
Available online 9 February 2009

Keywords:
Porous layer
Surface tension
Marangoni convection
Darcy–Benard–Marangoni convection

ABSTRACT

The onset of coupled Darcy–Benard–Marangoni convection in a liquid saturated porous layer of high permeability of practical importance is investigated by employing the Brinkman–Forchheimer– Lapwood-extended Darcy flow model with fluid viscosity different from effective viscosity. The lower boundary is taken to be rigid and insulating to temperature perturbations, while the upper surface is open to atmosphere and subject to a general thermal condition. The critical eigenvalues are obtained numerically, in general, using Galerkin method. However, closed form solution is also obtained using regular perturbation technique for insulated boundaries. Besides, the eigenvalue problem is solved exactly for pure Darcy–Marangoni convection. The numerical and analytical results are found to be in excellent agreement with each other. It is observed that the effect of buoyancy is destabilizing, while an increase in the permeability parameter is to delay the onset of convection. The Biot number and the ratio of effective viscosity to fluid viscosity are found to increase the critical conditions. Some known results are recovered as special cases.

1. Introduction

The convective instability in a horizontal fluid saturated porous layer heated from below is referred to as Darcy–Benard (DB) convection in which the instability is due to buoyancy forces. The DB convection has been studied extensively since the pioneering works of Horton and Rogers [1] and Lapwood [2] owing to its natural occurrence and also its importance in many scientific, engineering and technological applications. The copious literature covering different developments in this field are well documented in [3–9]. However, apart from the buoyancy forces, convective instability in a liquid saturated porous layer can also occur due to temperature dependent surface tension forces at the free surface contact with air known as Darcy–Marangoni (DM) convection. The study of DM convection has drawn little attention compared to DB convection in spite of its importance in materials science processing, solidification of alloys, etc.

Patberg et al. [10] have studied Marangoni effects in packed distillation columns. It is observed that large differences in refreshing of the liquid on wetted particles can be produced by Marangoni effect. White and Perroux [11] have examined experimentally that bulk liquid convection can be produced in porous media by macroscopic gradients in surface tension. In their seminal paper, Hennenberg et al. [12] have discussed in detail the Marangoni convection in a liquid saturated porous matrix. The Brinkman model of the porous medium and a representative elementary volume (rev) averaged surface tension at the upper layer of liquid- saturated porous medium with its upper surface in contact with air is considered in analyzing the problem. The critical Marangoni number for the onset of convection for different values of permeability parameter is determined. On the other hand, the effect of Brinkman boundary layer on the onset of convection in a porous layer driven by surface tension gradients at both the bounding free adiabatic surfaces has been studied by Rudraiah and Prasad [13]. In a comment on the paper by Hennenberg et al. [12], Nield [14] has suggested a composite fluid and porous layer model for the study of Marangoni convection in a porous layer. But Nield himself is doubtful about the suitability of the model (i.e., single porous layer or composite fluid layer overlying a porous layer) since experimental studies are lacking in this direction to dwell upon the situation on hand. Desaive et al. [15] have studied coupled capillary and gravity driven instability in a fluid layer overlying a porous layer using Brinkman's model to describe the flow in the porous medium. They have determined the critical Rayleigh and Marangoni number for the onset of convection. Saghir et al. [16] have developed a detailed numerical analysis to study the onset of a coupled Benard–Marangoni convection in a porous fluid combined layer bounded by vertical side walls. While Saghir et al. [17] have studied the onset of combined Marangoni and gravity driven convection in a liquid porous cavity of finite size subject to two different heating conditions: bottom and lateral heating. Recently, Shivakumara et al. [18] have obtained exact solution for

* Corresponding author. Tel.: +91 080 22961437; fax: +91 080 22219714.
E-mail address: isshivakumara@hotmail.com (I.S. Shivakumara).

0017-9310/$ - see front matter © 2009 Elsevier Ltd. All rights reserved.
doi:10.1016/j.ijheatmasstransfer.2008.09.038

Nomenclature

a	overall horizontal wave number, $\sqrt{\ell^2+m^2}$
A	ratio of heat capacities, $(\rho_0 c)_e/(\rho_0 c_p)_l$
Bi	Biot number, $(h_e d/k_e)_l$
c	specific heat
C_d	dimensionless Forchheimer coefficient
d	thickness of the porous layer
D	differential operator, d/dz
$\vec{g}$	acceleration due to gravity
h_e	effective heat transfer coefficient, $\phi h_l + (1-\phi)h_s$
K	permeability of the porous medium
k_e	effective thermal conductivity of the porous medium, $\phi k_l + (1-\phi)k_s$
l,m	wave numbers in the x and y- directions, respectively
Ma	Marangoni number, $\left(-\frac{\partial \gamma_e}{\partial T}\right)\frac{\Delta T d}{\mu \kappa_e}$
M_e	effective Marangoni number, Ma/Λ
p	pressure
Pr	Prandtl number, $\nu\phi/\kappa_e$
$\vec{q}$	seepage velocity vector, (u,v,w)
R	Rayleigh number, $\alpha g \Lambda T d^3/\nu\kappa_e$
R_e	effective Rayleigh number, R/Λ
t	time
T	temperature
x,y,z	Cartesian co-ordinates

Greek symbols

α	thermal expansion coefficient of fluid density
∇_h^2	horizontal Laplacian operator, $\partial^2/\partial x^2+\partial^2/\partial y^2$
∇^2	Laplacian operator, $\nabla_h^2+\partial^2/\partial z^2$
ϕ	porosity of the porous medium
γ_e	surface tension
κ_e	effective thermal diffusivity, $k_e/(\rho_0 c_p)_l$
Λ	ratio of viscosities, μ_e/μ
μ	dynamic viscosity
μ_e	effective viscosity
ν	kinematic viscosity, μ/ρ_0
θ	perturbed temperature
ρ	density
$(\rho_0 c)_e$	effective heat capacity of the porous medium, $\phi(\rho_0 c_p)_l + (1-\phi)(\rho_0 c)_s$
$(\rho_0 c_p)_l$	heat capacity of the liquid
$(\rho_0 c)_s$	heat capacity of the solid
σ	permeability parameter, $d/\sqrt{K}$
σ_e	effective permeability parameter, $\sigma/\sqrt{\Lambda}$

Subscripts

b	basic state
e	effective
l	liquid
s	solid
0	reference

the onset of surface-tension driven convection in superposed fluid and porous layers using the Darcy momentum law to study the fluid flow in the porous medium.

The existing theoretical studies are concerned only with Marangoni convection in porous media. Many experimental observations reveal that buoyancy forces, however small they may be, play a decisive role on convective processes even under the microgravity conditions. There exist several works on coupled Benard–Marangoni convection in a clear fluid layer (see Perez-Garcia and Carneiro [19], Char and Chiang [20], Bragard and Velarde [21], Or and Kelly [22] and references therein). But to our knowledge, its counterpart in a porous layer called Darcy–Benard–Marangoni (DBM) convection has not received any attention so far. For a high porosity porous medium, Givler and Altobelli [23] have demonstrated experimentally that the effective viscosity is about 7.5 times the fluid viscosity. Therefore, the aim of the present study is essentially to investigate the linear stability analysis of a more generalized problem of coupled DBM convection in a sparsely packed porous medium by employing the Brinkman–Forchheimer–Lapwood-extended–Darcy flow model with effective viscosity different from fluid viscosity. In the present work, the ratio of these two viscosities is taken as a separate parameter to know its influence on the critical stability parameters. Also, the values of the permeability parameter are suitably chosen in the range $\sqrt{0.1} \leqslant \sigma \leqslant \sqrt{10^3}$, where σ is the permeability parameter, as suggested by Walker and Homsy [24]. We consider the lower boundary as rigid and insulating to temperature perturbations, while the upper free boundary at which the surface tension acts is assumed to be governed by Newton's cooling law which very well represents the general situation. The present investigation also provides theoretical frame work in conducting experiments on DBM convection, which are lacking in this direction at present.

The paper is organized as follows. The basic equations and the boundary conditions are obtained in Section 2 on the lines outlined in Hennenberg et al. [12]. The eigenvalue problem is solved numerically, in general, using Galerkin method in Section 3. Besides, the eigenvalue problem is solved by regular perturbation technique when both boundaries are insulated to temperature perturbations and also exactly for pure DM convection in Sections 4 and 5, respectively. The results are discussed in Section 6, and conclusions drawn are presented in Section 7.

2. Mathematical formulation

We consider a Boussinesquian liquid saturated horizontal sparsely packed porous layer of thickness d with no lateral boundaries (see Fig. 1). The lower boundary is assumed to be rigid, while the upper free surface which is in contact with air and subjected to temperature-dependent surface tension forces is assumed to be flat and undeformable. A temperature difference of T is maintained between the boundaries of the porous layer with the lower boundary at a higher temperature than the upper boundary. A Cartesian coordinate system (x, y, z) is chosen such that the origin is at the lower boundary and the z axis is taken vertically upward. The gravity acts in the negative z direction, $\vec{g} = -g\hat{k}$, where $\hat{k}$ is the unit vector. The surface tension effects at the upper free surface of the liquid-saturated porous medium are due to both liquid–gas and

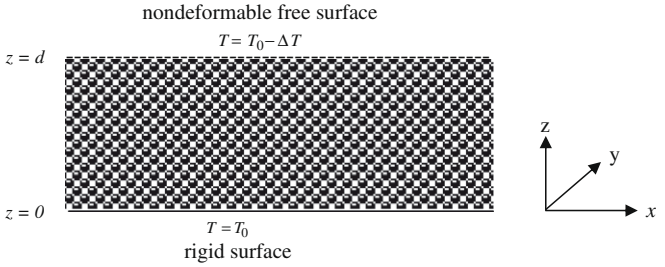

Fig. 1. Physical configuration.

solid–gas interfaces. Thus one has to consider the effective surface tension γ_e from a more complete description of the porous medium and the wetting liquid. However, in the present study we have adopted the Hennenberg et al. [12] contrivance in considering the surface tension effects and assume that γ_e is of the same order of magnitude as the liquid–gas one and has the same temperature dependence of the form (Pearson [25])

$$\gamma_e = \gamma_{e0} - \gamma_{eT}(T - T_0) \tag{1}$$

where γ_{e0} is the reference value and $-\gamma_{eT}$ is the rate of change of surface tension with temperature.

The fluid density ρ is assumed to vary linearly with temperature in the form

$$\rho = \rho_0\{1 - \alpha(T - T_0)\} \tag{2}$$

where α is the thermal expansion coefficient and ρ_0 is the density at $T = T_0$.

The continuity, momentum and energy equations are, respectively, given by (Nield and Bejan [9])

$$\nabla \cdot \vec{q} = 0 \tag{3}$$

$$\rho_0\left(\frac{1}{\phi}\frac{\partial \vec{q}}{\partial t} + \frac{1}{\phi^2}(\vec{q}\cdot\nabla)\vec{q}\right) = -\nabla p + \rho\vec{g} - \frac{\mu}{K}\vec{q} + \mu_e\nabla^2\vec{q} - \frac{\rho_0 C_d}{\sqrt{K}}|\vec{q}|\vec{q} \tag{4}$$

$$(\rho_0 c)_e\frac{\partial T}{\partial t} + (\rho_0 c_p)_l(\vec{q}\cdot\nabla)T = k_e\nabla^2 T \tag{5}$$

where the quantities appearing in the above equations are defined in the nomenclature.

The basic state is quiescent and is given by

$$\vec{q}_b = 0, \quad T_b = -\frac{\Delta T}{d}z + T_0, \quad p_b(z) = p_0 - \rho_0 g z - \alpha\rho_0 g\frac{\Delta T}{d}\frac{z^2}{2} \tag{6}$$

where the subscript b denotes the basic state. The pressure distribution is of no consequence here as we are going to eliminate the same. To study the stability of DBM convection, we superimpose infinitesimal disturbances on the basic state solution and substitute into the governing Eqs. (3)–(5). Employing the well known standard linear stability analysis procedure and eliminating the pressure from the momentum equation by operating curl twice and retaining the z-component, we arrive at the following dimensionless equations:

$$\left(\frac{1}{\mathrm{Pr}}\frac{\partial}{\partial t} + \sigma^2 - \Lambda\nabla^2\right)\nabla^2 w = R\nabla_h^2\theta \tag{7}$$

$$\left(A\frac{\partial}{\partial t} - \nabla^2\right)\theta = w \tag{8}$$

where, w is the z-component of perturbation velocity, θ is the perturbation temperature and $\nabla_h^2 = \partial^2/\partial x^2 + \partial^2/\partial y^2$ is the horizontal Laplacian operator. In the process of non-dimensionalization, we have employed d, $d^2/\kappa e$, κ_e/d and ΔT as the length, time, velocity and temperature scales, respectively. The non-dimensional numbers appearing in the above equations are: R the Rayleigh number, the Pr Prandtl number, σ the porous parameter, Λ the ratio of viscosities and A being the ratio of heat capacities.

The boundary conditions at the bottom are for a rigid boundary insulated to temperature perturbations:

$$w = \frac{\partial w}{\partial z} = \frac{\partial\theta}{\partial z}, \quad \text{at } z = 0. \tag{9}$$

The complex issue, however, is about imposing the conditions on the upper free surface at which surface tension effects are considered. This is based on rev averaged surface tension as detailed in the work of Hennenberg et al. [12]. The boundary conditions at the top surface are

$$w = \frac{\partial\theta}{\partial z} + Bi\theta = 0 \quad \text{at } z = 1 \tag{10}$$

where Bi is the Biot number, and the balance between shear stresses and the surface tension gradients (Pearson [25]) conditions, on using Eq. (2), give

$$\frac{\partial u}{\partial z} = -\frac{Ma}{\Lambda}\frac{\partial\theta}{\partial x} \quad \text{at } z = 1 \tag{11a}$$

$$\frac{\partial v}{\partial z} = -\frac{Ma}{\Lambda}\frac{\partial\theta}{\partial y} \quad \text{at } z = 1 \tag{11b}$$

where Ma is the Marangoni number. Eqs. (11a) and (11b) are differentiated partially with respect to x and y, respectively, and the results are added to get, after using Eq. (3), the following condition:

$$\frac{\partial^2 w}{\partial z^2} = M_e\nabla_h^2\theta \quad \text{at } z = 1 \tag{12}$$

where $M_e = Ma/\Lambda$ is the effective Marangoni number. It may be noted here that the above surface tension condition slightly differs from that used by Hennenberg et al. [12] This is due to the fact that we have taken the ratio of viscosities as a separate parameter rather than expressing it in terms of tortuosity.

We seek solution for w, and θ in terms of normal modes of the form

$$(w, \theta) = [W(z), \Theta(z)]\exp\{i(\ell x + my) + \omega t\} \tag{13}$$

where l and m are wave numbers in the x and y directions, respectively, and ω is the complex growth rate of the disturbances. Substituting Eq. (13) into Eqs. (7) and (8) and noting from the previous analyses that the principle of exchange of stability holds (see Hennenberg et al. [12], Rudraiah and Prasad [13]), we obtain the following equations relevant to neutral stability:

$$\left[(D^2 - a^2)^2 - \sigma_e^2(D^2 - a^2)\right]W = \mathrm{R}_e a^2\Theta \tag{14}$$

$$(D^2 - a^2)\Theta = -W \tag{15}$$

where $a = \sqrt{l^2 + m^2}$ is the overall horizontal wave number, $D = d/dz$ is the differential operator, $\sigma_e = \sigma/\sqrt{\Lambda}$ is the effective porous parameter and $R_e = R/\Lambda$ is the effective Rayleigh number. The boundary conditions given by Eqs. (9), (10), and (12) on using Eq. (13), become

$$W = DW = D\Theta = 0 \quad \text{at} \quad z = 0. \tag{16}$$

$$W = D^2W + M_e a^2\Theta = D\Theta + Bi\Theta = 0 \quad \text{at } z = 1. \tag{17}$$

3. Numerical solution

Eqs. (14) and (15) together with the boundary conditions given by Eqs. (16) and (17) constitute an eigenvalue problem with M_e or R_e as the eigenvalue. The Galerkin method is employed to solve the eigenvalue problem as explained in the book by Finlayson [26]. Accordingly, the unknown variables are written in a series of basis functions as

$$W = \sum_{i=1}^{n} A_i W_i, \quad \Theta = \sum_{i=1}^{n} B_i\Theta_i \tag{18}$$

where A_i and B_i are constants and the basis functions W_i and Θ_i will be represented by the power series satisfying the boundary conditions. Substituting Eq. (18) into Eqs. (14) and (15) and the Galerkin procedure of demanding the residues be orthogonal to the basis functions are applied, we get the following system of homogeneous algebraic equations.

$$C_{ji}A_i + D_{ji}B_i = 0 \tag{19a}$$

$$E_{ji}A_i + F_{ji}B_i = 0. \tag{19b}$$

The coefficients C_{ji} to F_{ji} involve inner products of the basis functions and are given by

$$C_{ji} = < D^2W_jD^2W_i + (2a^2+\sigma_e^2)DW_jDW_i + a^2(a^2+\sigma_e^2)W_jW_i > \quad (20a)$$

$$D_{ji} = -R_e a^2 < W_j\Theta_i > + a^2 M_e DW_j(1)\Theta_i(1) \quad (20b)$$

$$E_{ji} = - < \Theta_j W_i > \quad (20c)$$

$$F_{ji} = Bi\Theta_j(1)\Theta_i(1) + < D\Theta_j D\Theta_i + a^2\Theta_j\Theta_i > \quad (20d)$$

where the inner product is defined as $< fg >= \int_0^1 fg dz$.

The system of homogeneous equations given by Eq. (19a) will have a nontrivial solution if and only if

$$\begin{vmatrix} C_{ji} & D_{ji} \\ E_{ji} & F_{ji} \end{vmatrix} = 0. \quad (21)$$

The inner products involved in Eq. (20a) are evaluated analytically to avoid errors in the numerical integration by choosing modified Tchebyshev polynomials as trial functions. For a fixed value of R_e, σ_e and Bi, the above characteristic equation gives a relation between M_e and wave number a enabling us to plot a locus in the $M_e - a$ plane. The minimum point of M_e as a function of wave number a gives the critical effective Marangoni number M_{ec} and the corresponding critical wave number a_c. This procedure is repeated for different values of R_e, σ_e, Bi and the results are discussed in Section 6.

4. Closed form solution by regular perturbation technique

When both boundaries are insulating to temperature perturbations (i.e., $D\Theta = 0$ at $z = 0, 1$) the critical wave number is negligibly small. This assumption, however, is not on physical guess based on previous results but the numerical calculations which are carried out in the previous section also corroborate this result. Once we realize this fact, the eigenvalue problem can now be solved by regular perturbation technique with wave number a as a perturbation parameter (Nield [27] and Garcia-Ybarra et al. [28]). Accordingly, the variables W and Θ are expanded in powers of a^2 as

$$(W, \Theta) = \sum_{i=0}^{n} a^{2i}(W_i, \Theta_i). \quad (22)$$

Substituting Eq. (22) into Eqs. (14) and (15) and also in the boundary conditions (16) and (17) collecting the terms of zeroth order, we obtain

$$D^4W_0 - \sigma_e^2 D^2W_0 = 0 \quad (23a)$$

$$D^2\Theta_0 = -W_0 \quad (23b)$$

with the boundary conditions

$$W_0 = DW_0 = 0 = D\Theta_0 \quad \text{at } z = 0 \quad (24a)$$

$$W_0 = D^2W_0 = 0 = D\Theta_0 \quad \text{at } z = 1. \quad (24b)$$

The solution to the zeroth order equations is given by

$$W_0 = 0 \quad \text{and} \quad \Theta_0 = 1. \quad (25a)$$

The first order equations are then

$$D^4W_1 - \sigma_e^2 W_1 = \mathrm{R}_e, \quad (25b, c)$$

$$D^2\Theta_1 = 1 - W_1 \quad (25b, d)$$

with the boundary conditions

$$W_1 = DW_1 = 0 = D\Theta_1 \quad \text{at } z = 0 \quad (26a)$$

$$W_1 = D^2W_1 + M_e = 0 = D\Theta_1 \quad \text{at } z = 1. \quad (26b)$$

The solution of Eq. (25b) subject to the above boundary conditions is given by

$$W_1 = c_1 + c_2 z + c_3\cosh(\sigma_e z) + c_4\sinh(\sigma_e z) - \mathrm{R}_e z^2/2\sigma_e^2 \quad (27a)$$

where the arbitrary constants c_1–c_4 are found to be

$$c_1 = \frac{\mathrm{R}_e\{(\sigma_e^2-2)\sinh\sigma_e + 2\sigma_e\}}{2\sigma_e^4(\sinh\sigma_e - \sigma_e\cosh\sigma)} + \frac{M_e(\sinh\sigma_e - \sigma_e)}{\sigma_e^2(\sinh\sigma_e - \sigma\cosh\sigma_e)} \quad (27b)$$

$$c_2 = -\frac{\mathrm{R}_e\{(\sigma_e^2-2)\cosh\sigma_e + 2\}}{2\sigma_e^3(\sinh\sigma_e - \sigma_e\cosh\sigma_e)} - \frac{M_e(\cosh\sigma_e - 1)}{\sigma_e(\sinh\sigma_e - \sigma_e\cosh\sigma_e)} \quad (27c)$$

$$c_3 = -c_1, \quad c_4 = -c_2/\sigma_e. \quad (27d, e)$$

From Eq. (25b,d), it follows that

$$1 = \int_0^1 W_1 dz. \quad (28)$$

Substituting for W_1 from Eq. (27a) in Eq. (28) and carrying out the integration leads to an expression of the form

$$1 = R_{ec}\frac{\{4\sigma_e(\sigma_e^2-6)\sinh\sigma_e + (24-\sigma_e^4)\cosh\sigma_e + 12(\sigma_e^2-2)\}}{12\sigma_e^5(\sinh\sigma_e - \sigma_e\cosh\sigma_e)} + M_{ec}\frac{\{4\sigma_e\sinh\sigma_e - (\sigma_e^4+4)\cosh\sigma_e - \sigma_e^2 + 4\}}{2\sigma_e^3(\sinh\sigma_e - \sigma_e\cosh\sigma_e)}. \quad (29)$$

It is interesting to check Eq. (29) for existing results in the literature under some limiting cases. In the absence of surface tension forces (i.e., $M_{ec} = 0$), the above equation reduces to

$$R_{ec} = \frac{12\sigma_e^5(\sinh\sigma_e - \sigma_e\cosh\sigma_e)}{\{4\sigma_e(\sigma_e^2-6)\sinh\sigma_e + (24-\sigma_e^4)\cosh\sigma_e + 12(\sigma_e^2-2)\}}. \quad (30)$$

The solution given by Eq. (30) is exact and coincides with the one obtained by Vasseur et al. [29] as a limit of the system fluid layer over a porous layer and also with Shivakumara and Nanjundappa [30]. From Eq. (30) the following results can be deduced.

As $\sigma_e \to 0$ (i.e., in the absence of a porous medium)

$$R_{ec} \sim 320\left(1 + \frac{\sigma_e^2}{21}\right) \quad (31)$$

and the result $R_{ec} = 320$ is the known exact value for the fluid layer case [24].

Also, as $\sigma_e \to \infty$ (i. e. Darcy case)

$$R_{eDc} = \frac{R_{ec}}{\sigma_e^2} \sim 12 + \frac{36}{\sigma_e} \quad (32)$$

where, $R_{eD} = R_e/\sigma_e^2$ is the Darcy-Rayleigh number and the result $R_{eDc} = 12$ is the known exact value for the densely packed porous layer [9]. The term $36/\sigma_e$ represents the boundary layer correction. In the absence of buoyancy forces (i.e., $R_{ec} = 0$), Eq. (29) simply reduces to

$$M_{ec} = \frac{2\sigma_e^3(\sinh\sigma_e - \sigma_e\cosh\sigma_e)}{\{4\sigma_e\sinh\sigma_e - (\sigma_e^4+4)\cosh\sigma_e - \sigma_e^2 + 4\}} \quad (33)$$

and this is the exact solution for Marangoni convection in a porous layer.

We note that as $\sigma_e \to 0$,

$$M_{ec} \sim 48\left(1 + \frac{\sigma_e^2}{20}\right). \quad (34)$$

The result $M_{ec} = 48$ is the known exact value for a clear liquid layer [21].

As $\sigma_e \to \infty$,

$$M_{eDc} = \frac{M_{ec}}{\sigma_e^2} \sim 2 + \frac{6}{\sigma_e} \quad (35)$$

where $M_{eD} = M_e/\sigma_e^2$ is the effective Darcy–Marangoni number. The second term $6/\sigma_e$ represents the boundary layer correction.

5. Exact solution for DM convection

If the convective instability in a porous layer is considered to be solely due to surface tension forces (i.e., $R_e = 0$) then the eigenvalue

problem for DM convection can be solved exactly. The aim of the present section is to explore this possibility. The method of solution also helps in knowing the accuracy of the results obtained from the previous methods, particularly with those obtained by regular perturbation technique. Since $R_e = 0$, Eq. (14) can now be solved directly to get

$$W = A_1[\cosh(az) + b\beta\sinh(az) - \cosh(bz) - a\beta\sinh(bz)] \tag{36a}$$

where,

$$b^2 = a^2 + \sigma_e^2, \quad \beta = \frac{\cosh b - \cosh a}{(b\sinh a - a\sinh b)} \tag{36b, c}$$

and A_1 is a constant.

Substituting for W thus obtained in Eq. (15) and solving, we obtain

$$\Theta = A_1\left[\delta_1\cosh(az) + \delta_2\sinh(az) - \frac{1}{2a}z\sinh(az) - \frac{b\beta}{2a}z\cosh(az) + \frac{1}{\sigma_e^2}\cosh(bz) + \frac{a\beta}{\sigma_e^2}\sinh(bz)\right] \text{where,} \tag{37a}$$

$$\delta_1 = \frac{1}{2a^2\sigma_e^2(a\sinh a + Bi\cosh a)}\left[\sinh a\{b\beta\sigma_e^2(a^2 - Bi) + a\sigma_e^2 + aBi(\sigma_e^2 + 2ab\beta\}) + \cosh a\{ab\beta(\sigma_e^2 Bi + 2a^2) + a^2\sigma_e^2\} - 2a^2\sinh b(b + a\beta Bi) - 2a^2\cosh b(ab\beta + Bi)\right] \tag{37b}$$

$$\delta_2 = \frac{(\sigma_e^2 - 2a^2)b\beta}{2a^2\sigma_e^2}. \tag{37c}$$

Utilizing the expressions for W and Θ given by Eqs. (36a) and (37a), respectively, in the coupled boundary condition

$$M_e a^2\Theta(1) = -D^2W(1) \tag{38}$$

we obtain an exact formula for M_e in the form

$$M_e = \frac{2\sigma_e^2[b^2\cosh b - a^2\cosh a + ab\beta(b\sinh b - a\sinh a)]}{[2a^2\cosh b + 2a^3\beta\sinh b + \eta_1\cosh a + \eta_2\sinh a]} \text{ where,} \tag{39a}$$

$$\eta_1 = a\sigma_e^2(2a\delta_1 - b\beta) \tag{39b}$$

$$\eta_2 = a\sigma_e^2(2a\delta_2 - 1) \tag{39c}$$

6. Results and discussion

The eigenvalue is taken to be either effective Marangoni number M_e or effective Rayleigh number R_e as the case may be. The critical eigenvalue (M_{ec} or R_{ec}) and the corresponding wave number (a_c) obtained both numerically as well as analytically in some cases are presented graphically in Figs. 2–5 for different values of R_e or M_e, σ_e and Bi. For many porous materials of scientific and technological importance, the permeability of the porous medium is very high and accordingly the values of the permeability parameter σ are chosen. In order to have a check on the accuracy of the numerical method used, first test computations are carried out for different values of Bi varying between zero and infinity with, $\Lambda = 1$, $M_e = 0$ and $\sigma_e = 0$ (i.e., in the absence of porous medium or classical viscous case). The critical Rayleigh numbers and wave numbers thus obtained are compared with those of Sparrow et al. [31] in Table 1. From the Table 1 we note that there is a very good agreement between both the approaches and thus verifies the accuracy of the method used. Also, an increase in the value of Biot number is to increase the critical Rayleigh and wave numbers and thus its effect is to delay the onset of convection as well as to reduce the dimension of convection cells. This may be due to the fact that with an increase in Bi the free surface deviates from good conductor and hence there is an increase in the critical stability parameters.

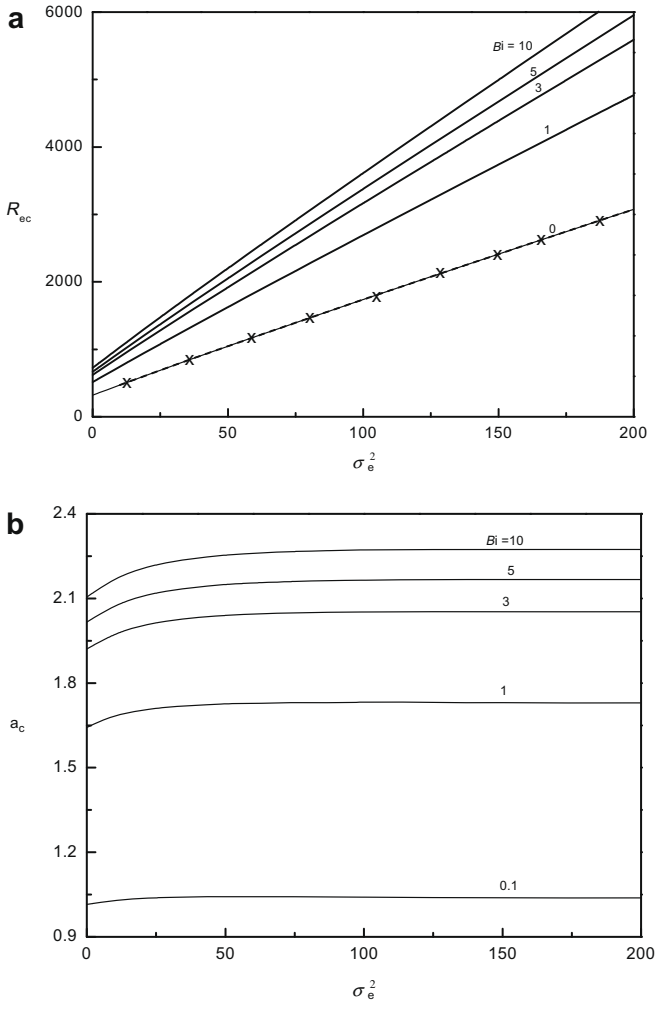

Fig. 2. Plots of (a) effective critical Rayleigh number R_{ec}, and (b) effective critical wave number a_c versus the square of effective permeability parameter σ_e^2 for different values of Biot number Bi when the effective Marangoni number $M_e = 0$. The numerical (—) and regular perturbation (——) solutions completely coincide for $Bi = 0$.

The results for DB and DM convection, obtained from the present study as particular cases, and also for coupled DBM convection are separately discussed in the following sub-sections.

6.1. DB convection

In this case, the convective instability is only due to buoyancy forces and take $M_e = 0$. The numerically calculated critical effective Rayleigh number R_{ec} and the corresponding wave number a_c are shown in Figs. 2(a) and 2(b), respectively, as a function of σ_e for different values of Bi. Fig. 1(a) indicates that increase in σ_e and Bi is to delay the onset of convection. It is also seen that deviation in R_{ec} values goes on decreasing with an increase in the value of Bi (>1). Although the increase in a_c is slow for $\sigma_e^2 \leqslant 50$, the critical wave number remains practically constant with further increase in σ_e for all values of Bi considered. However, increase in Bi is to increase a_c and thus its effect is to decrease the dimensions of the convective cell. For $Bi = 0$ (i.e., when both boundaries are insulating to temperature perturbations), a_c is found to be negligibly small suggesting the unicellular pattern of convection. This fact has been exploited to find a closed form analytical solution for the onset of convection by regular perturbation technique. The critical effective Rayleigh number so obtained is also shown in Fig. 2(a) by dashed lines. We

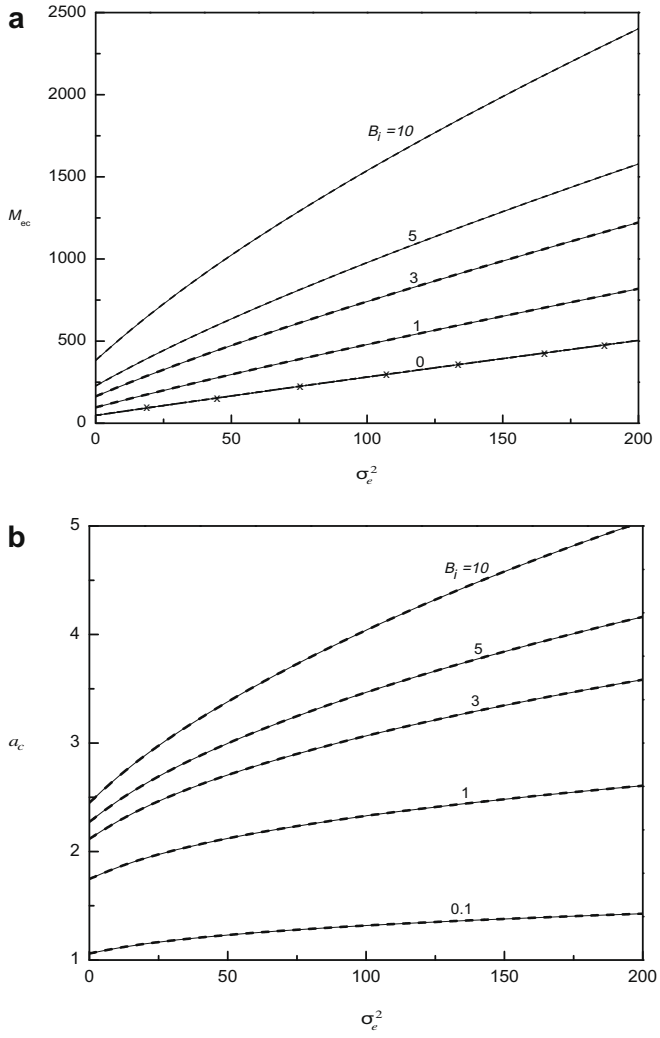

Fig. 3. Plots of (a) critical effective Marangoni number M_{ec}, and (b) effective critical wave number a_c versus square of effective permeability parameter σ_e^2 for different values of Biot number Bi when the effective Rayleigh number $R_e = 0$. The numerical (—), exact (----) and regular perturbation (——) solutions completely coincide.

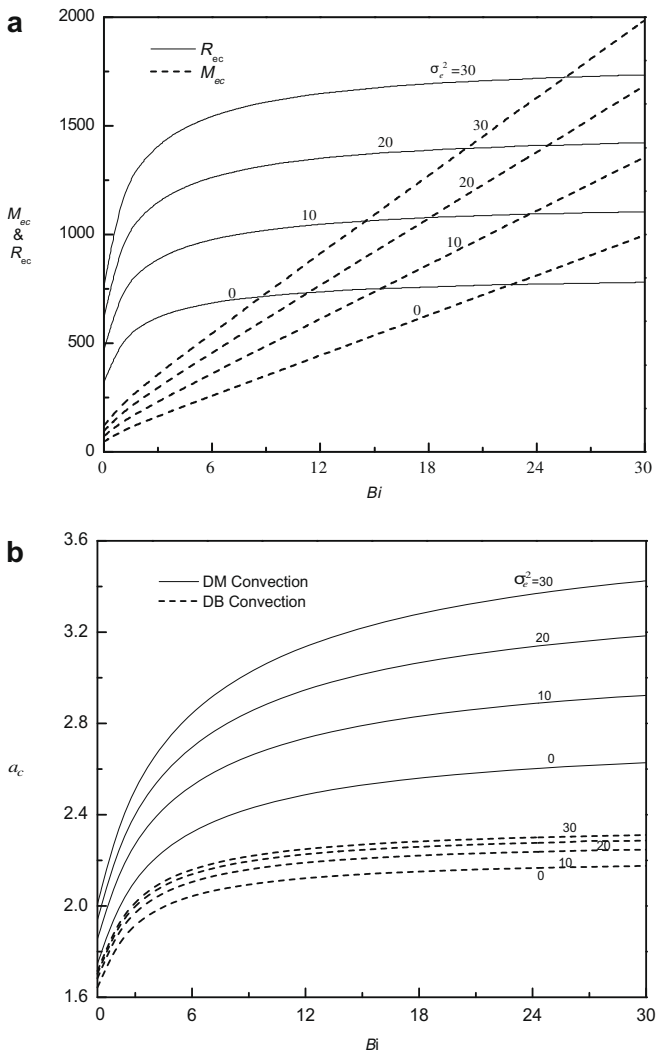

Fig. 4. Plots of (a) effective critical Marangoni number M_{ec} and Rayleigh number R_{ec}, and (b) effective critical wave number a_c versus Biot number Bi for different values of effective permeability parameter σ_e.

note that the critical Rayleigh numbers coincide with each other suggesting the solution obtained for insulated boundaries by regular perturbation technique is not an approximate one instead it is exact.

6.2. DM convection

We consider here that the convective instability is only due to surface tension forces and take $R_e = 0$. Fig. 3(a) and (b) show the variation of M_{ec} and a_c with σ_e for different values of Bi. As already noted in DB convection, the effect of increase in σ_e and Bi is to delay the onset of DM convection as well (see Fig. 3(a)). When $Bi = 0$, a_c is again found to be vanishingly small and the regular perturbation technique is used to obtain an analytical expression for M_{ec}. Besides, an exact solution for the eigenvalue problem is also obtained. The values of M_{ec} and a_c calculated from the exact formula (cf. Eq. (39a)) are also indicated in Fig. 3 by dashed lines. We note that the results obtained from numerical and analytical methods compare very well with each other. In particular, the solution obtained by regular perturbation technique for $Bi = 0$ coincides with the exact solution and thereby reconfirms the solution given by Eq. (30) is exact. Both Ma_c and a_c values obtained numerically as well as by exact analysis for different values of Bi with $\sigma_e = 0$ (i.e., in the absence of porous medium or classical viscous case) are tabulated in Table 2. From the Table 2 it is seen that the results computed numerically are in excellent agreement with those obtained under exact analysis. The effect of increase in the Biot number is to delay the onset of Marangoni convection and also to reduce the dimension of convection cells as observed in the previous case (see Table 1).

A glance at the critical eigenvalues M_{ec} and R_{ec} presented in Fig. 4(a) as a function of Bi for different values of σ_e reveals that $M_{ec} < R_{ec}$ up to a certain range of values of Bi; exceeding which an opposite type of behavior could be seen (see also Tables 1 and 2). Further, it is evident that an increase in the value of σ_e is to increase the range of Bi up to which $M_{ec} < R_{ec}$. Also, the variation in R_{ec} is negligible for the values of Bi considered, but M_{ec} increases significantly with Bi. The critical wave numbers for DM convection are always found to be higher than those for DB convection (see Fig. 4(b)). This may be due to the fact that the effect of surface tension force is to contract the surface and in turn to shrink the convective cells.

6.3. DBM convection

The effects of both gravity and surface tension forces are considered together in the discussion. The effective critical Marangoni

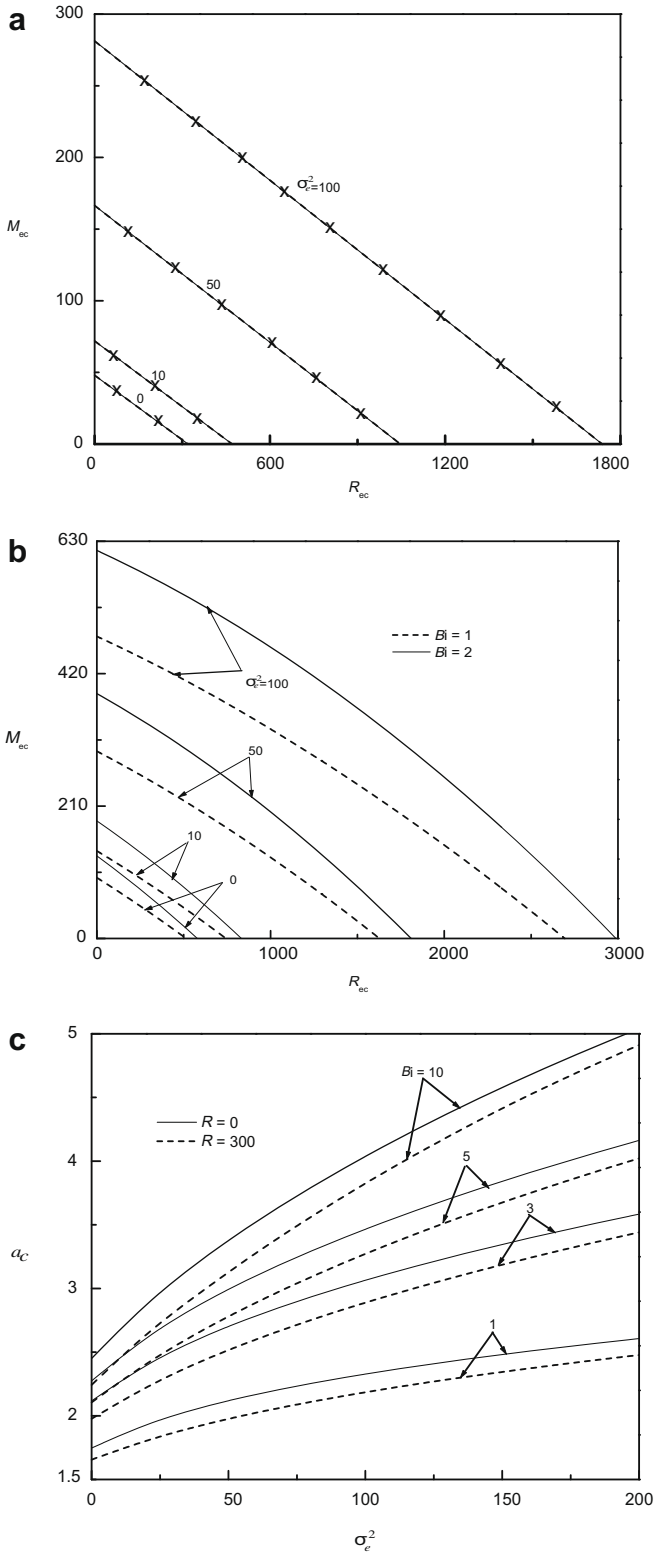

Fig. 5. Locus of critical effective Marangoni number M_{ec} and effective Rayleigh number R_{ec} for (a) $Bi = 0$, and (b) $Bi = 1$ and 2 for different values of permeability parameter σ_e^2. The numerical (—) and regular perturbation (- - - -) solutions completely coincide for $Bi = 0$. (c). Plots of critical wave number a_c versus square of effective permeability parameter σ_e^2 for different values of Biot number Bi.

and Rayleigh numbers obtained numerically for different values of σ_e which are shown in Fig. 5(a) for $Bi = 0$ and in Fig. 5(b) for $Bi = 1$ and 2. Even in the present case, it is observed that the critical wave number is negligibly small when $Bi = 0$ and the solution given by

Table 1
Comparison of critical Rayleigh number R_c and critical wave number a_c for different values of Bi with $M_e = 0$ and $\sigma_e = 0$ (i.e., in the absence of a porous medium).

Bi	Sparrow et al. [31]		Present study	
	R_c	a_c	R_c	a_c
0	320.000	0.00	320.000	-2.641×10^{-9}
0.01	338.905	0.58	338.904	0.5831
0.03	353.176	0.76	353.158	0.7624
0.1	381.665	1.015	381.665	1.0151
0.3	428.290	1.03	428.290	1.2992
1	513.792	1.64	513.790	1.6438
3	619.666	1.92	619.666	1.9211
10	725.150	2.11	725.147	2.1055
30	780.240	2.18	780.237	2.1760
100	804.973	2.20	804.972	2.2029
∞	816.748	2.21	816.744	2.2147

Table 2
Critical values of Marangoni number Ma_c and wave number a_c for various values of Bi with $R = 0$ and $\sigma_e = 0$ (i.e., in the absence of a porous medium).

Bi	Numerical solution		Exact solution	
	Ma_c	a_c	Ma_c	a_c
0	48.000	3.4246×10^{-9}	48.000	0.000
0.01	50.710	0.6129	50.710	0.6136
0.03	52.988	0.7987	52.988	0.7997
0.1	58.151	1.0603	58.150	1.0603
0.3	68.534	1.3593	68.534	1.3599
1	96.338	1.7474	96.336	1.7474
3	163.905	2.1180	163.902	2.1167
10	383.186	2.4506	383.185	2.4500
30	995.988	2.6286	995.986	2.6300
100	3131.680	2.7129	3131.670	2.7128
∞	3.0490×10^{19}	2.7544	3.0438×10^{19}	2.7545

Eq. (29) is exact. The results obtained by regular perturbation technique for different values of σ_e are also presented in Fig. 5(a) and note that the results agree very well with the numerical ones. In these figures, the regions above and below M_{ec} versus R_{ec} curves, correspond, respectively, to stable and unstable ones. It is observed that there is a strong coupling between M_{ec} and R_{ec} such that an increase in one decreases the other. That is, increase in the buoyancy force decreases the effect of surface tension force on the onset of convection and vice-versa. Moreover, increase in σ_e and Bi is to increase the region of stability. From Fig. 5(a) and (b) it is also evident that the stability curves are straight lines for $Bi = 0$ (see Fig. 5(a)), whereas they are slightly convex for values of $Bi = 1$ and 2 (see Fig. 5(b)). In particular, from Eq. (29), it is noted that

$$1 = \frac{R_{ec}}{320(1+\sigma_e^2/21)} + \frac{M_{ec}}{48(1+\sigma_e^2/20)} \quad \text{as } \sigma_e \to 0 \text{ and} \tag{40a}$$

$$1 = \frac{R_{eDc}}{12(1+3/\sigma_e)} + \frac{M_{eDc}}{2(1+3/\sigma_e)} \quad \text{as } \sigma_e \to \infty. \tag{40b}$$

The variation of critical wave number a_c as a function of σ_e^2 is shown in Fig. 4(c) for two values of $R_e = 0$ and 300 with different values of Bi. From the figure it is seen that increase in σ_e and Bi is to increase a_c. On the contrary, the presence of buoyancy force is to decrease the critical wave number. The critical Marangoni and wave numbers obtained numerically for different values of Λ, Bi and σ^2 for two values of $R = 0$ and 200 are presented in Table 3. From the table we note that an increase in the value of Λ is to increase the critical Marangoni number and thus making the system more stable. Nevertheless, increase in Λ is to decrease the critical wave number, except for $Bi = 0$, and hence its effect is to increase the dimension of convection cells. Further, increase in Bi and σ is to make the system more stable, while an increase in the Rayleigh number R makes the system unstable.

Table 3
Comparison of critical Marangoni number Ma_c and critical wave number a_c for different values of Bi, Λ and σ^2.

R	Bi	σ^2	$\Lambda = 1$		$\Lambda = 3$		$\Lambda = 5$	
			Ma_c	a_c	Ma_c	a_c	Ma_c	a_c
0	0	10	71.974	0.000	167.997	0.000	263.999	0.000
		50	166.431	0.000	263.693	0.000	359.873	0.000
		100	281.212	0.000	382.189	0.000	479.172	0.000
	1	10	138.862	1.856	332.196	1.787	524.868	1.772
		50	297.041	2.122	499.196	1.913	694.310	1.856
		100	479.214	2.330	698.949	2.029	899.783	1.940
	5	10	318.279	2.467	775.783	2.344	1231.580	2.316
		50	635.814	2.998	1126.510	2.575	1591.400	2.476
		100	978.212	3.467	1530.520	2.805	2016.590	2.674
200	0	10	41.373	0.000	137.773	0.000	233.861	0.000
		50	134.627	0.000	232.789	0.000	329.272	0.000
		100	248.842	0.000	350.741	0.000	448.138	0.000
	1	10	104.582	1.770	297.688	1.757	490.458	1.754
		50	267.177	2.022	466.567	1.879	660.967	1.835
		100	453.023	2.231	668.167	1.994	867.677	1.918
	5	10	263.368	2.331	719.401	2.230	1174.880	2.289
		50	596.162	2.854	1076.690	2.525	1538.870	2.4737
		100	949.168	3.339	1487.160	2.755	1968.560	2.595

7. Conclusions

The onset of coupled DBM convection in a highly permeable porous medium of scientific and technological importance is investigated. The lower boundary is assumed to be rigid and insulated to temperature perturbations whereas the upper boundary is free with temperature dependent surface tension. Further, the heat transfer on the free boundary is described by a more general Newton's law of cooling with Biot number varying between zero and infinity. The eigenvalue problem is solved numerically, in general, using Galerkin method. For insulated boundaries, the convection occurs at a vanishingly small wave number and the solution to the eigenvalue problem obtained by regular perturbation technique is exact. Besides, an exact analysis is also being carried out to find M_e when the instability is only due to surface tension forces. It is noted that the critical eigenvalues obtained from a combination of analytical and numerical techniques complement very closely with each other. A comparison between the critical stability parameters of DB and DM convection discussed separately shows that there exists a critical value of Bi (depending on the value of permeability parameter σ_e) such that below which $M_{ec} < R_{ec}$, and above which $M_{ec} > R_{ec}$. However, the critical wave numbers for DM convection are always found to be higher than those for DB convection. The locus of (M_{ec}, R_{ec}) for different values of σ_e shows that it is a straight line for $Bi = 0$, while it is slightly convex for $Bi = 1$ and 2. The effect of increase in σ_e, Λ and Bi is to delay the onset of convection. Further, increase in σ_e and Bi, and decrease in Λ is to decrease the dimensions of the convective cell. Also, M_{ec} and a_c decrease with an increase in the Rayleigh number and thus the buoyancy force has a destabilizing effect on the system.

Acknowledgements

This work was supported by the UGC-Centre for Advanced Studies in Fluid Mechanics. The authors C.E.N. and K.B.C. thank the Management of their respective institutes for encouragement.

References

[1] C.W. Horton, G.T. Rogers, Convection current in a porous medium, J. Appl. Phys. 16 (1945) 367–370.
[2] E.R. Lapwood, Convection of a fluid in a porous medium, Proc. Camb. Philos. Soc. 44 (1948) 508–521.
[3] M. Kaviany, Principles of Heat Transfer in Porous Media, second ed., Springer-Verlag, New York, 1995.
[4] D.B. Ingham, I. Pop (Eds.), Transport Phenomena in Porous Media, Pergamon, Oxford, 1998.
[5] K. Vafai (Ed.), Hand Book of Porous Media, Marcel Dekker, New York, 2000.
[6] K. Vafai (Ed.), Handbook of Porous Media, second ed., Taylor and Francis (CRC), Boca Raton, 2005.
[7] A. Bejan I. Dincer, S. Lorente, A.F. Miquel, A.H. Reis, A.H. (Eds.), Porous and Complex Flow Structures in Modern Technologies, Springer, New York, 2004.
[8] Ingham, A. Bejan, E. Mamut, I. Pop (Eds.), Emerging Technologies and Techniques in Porous Media, Kluwer, Dordrecht, 2004.
[9] D.A. Nield, A. Bejan, Convection in Porous Media, third ed., Springer-Verlag, New York, 2006.
[10] B. Patberg, A. Kores, W.D.E. Steenge, A.A.H. Drinkenburg, Effectiveness of mass transfer in a packed distillation column in relation to surface tension gradients, Chem. Eng. Sci. 38 (1983) 917–923.
[11] I. White, K.M. Perroux, Marangoni instabilities in porous media, in: R.A. Wooding, I. White (Eds.), Proceedings of the CSIRO/DSIR Seminar on Convective Flows in Porous Media, DSIR, Wellington, New Zealand, 1985, pp. 99–111.
[12] M. Hennenberg, M.Z. Saghir, A. Rednikov, J.C. Legros, Porous media and the Benard–Marangoni problem, Trans. Porous Media 27 (1997) 327–355.
[13] N. Rudraiah, V. Prasad, Effect of Brinkman boundary layer on the onset of Marangoni convection in a fluid saturated porous layer, Acta Mech. 127 (1998) 235–246.
[14] D.A. Nield, Modelling the effect of surface tension on the onset of natural convection in a saturated porous medium, Trans. Porous Media 31 (1998) 365–368.
[15] T.H. Desaive, G. Lebon, M.H. Hennenberg, Coupled capillary and gravity driven instability in a liquid film overlying a porous layer, Phys. Rev. E 64 (2001) 66304–66308.
[16] M.Z. Saghir, P. Comi, M. Mehrvar, Effects of interaction between Rayleigh and Marangoni convection in a superposed fluid layer, Int. J. Thermal Sci. 41 (2002) 207–215.
[17] M.Z. Saghir, P. Mahendran, M. Hennenberg, Marangoni and gravity driven convection in a liquid layer overlying a porous layer: lateral and bottom heating conditions, Energy Sources 27 (2005) 151–171.
[18] I.S. Shivakumara, S.P. Suma, Krishna B. Chavaraddi, Onset of surface-tension-driven convection in superposed fluid and porous layers, Arch. Mech. 58 (2006) 71–92.
[19] C. Perez-Garcia, G. Carneiro, Linear stability analysis of Benard–Marangoni convection in fluids with a deformable free surface, Phys. Fluids 3 (2) (1991) 292–298.
[20] M.I. Char, K.T. Chiang, Stability analysis of Benard–Marangoni convection in fluids with internal heat generation, J. Phys. D 27 (1994) 748–755.
[21] J. Bragard, M.G. Velarde, Benard–Marangoni planforms and related theoretical predictions, J. Fluid Mech. 368 (1998) 165–194.
[22] A.C. Or, R.E. Kelly, The effects of thermal modulation upon the onset of Marangoni–Bernard convection, J. Fluid Mech. 456 (2002) 161–182.
[23] R.C. Givler, S.A. Altobelli, Determination of the effective viscosity for the Brinkman–Forchheimer flow model, J. Fluid Mech. 258 (1994) 355–361.
[24] K. Walker, G.M. Homsy, A note on convective instabilities in Boussinesq fluids and porous media, Trans. ASME 99 (1977) 338–339.
[25] J.R.A. Pearson, On convection cells induced by surface tension, J. Fluid Mech. 4 (1958) 489–500.
[26] B.A. Finlayson, Method of Weighted Residuals and Variational Principles, Academic press, 1972.
[27] D.A. Nield, Onset of convection in a fluid layer overlaying layer of porous medium, J. Fluid Mech. 81 (1977) 513–522.

[28] P.L. Garcia-Ybarra, J.L. Gastillo, M.G. Velarde, A nonlinear evolution for Benard–Marangoni convection with deformable boundary, Phys. Lett. A 122 (1987) 107–110.
[29] P. Vasseur, C.H. Wang, M. Sen, Thermal instability and natural convection in a fluid layer over a porous substrate, Wärme-und Stoffübertragung 24 (1989) 337–347.
[30] I.S. Shivakumara, C. E Nanjundappa, Onset of convection in a sparsely packed porous layer with throughflow, Arch. Mech. 53 (2001) 1–23.
[31] E.M. Sparrow, R.J. Goldstein, V.K. Jonsson, Thermal instability in a horizontal fluid layer: effect of boundary conditions and non-linear temperature profiles, J. Fluid Mech. 18 (1964) 513–528.